Available online at www.sciencedirect.com
ScienceDirect
Scripta Materialia 63 (2010) 605–608
Scripta MATERIALIA
www.elsevier.com/locate/scriptamat

Phase evolution and photoluminescence in as-deposited amorphous silicon nitride films

Sarab Preet Singh,[a] P. Srivastava,[a] S. Ghosh,[a] S.A. Khan,[b] Claudio J. Oton[c,1] and G. Vijaya Prakash[a,*]

[a] *Nanostech and Nanophotonics Laboratories, Department of Physics, Indian Institute of Technology Delhi, Hauz Khas, New Delhi 110 016, India*
[b] *Inter-University Accelerator Centre, Aruna Asif Ali Marg, New Delhi 110 067, India*
[c] *Optoelectronics Research Centre, University of Southampton, Southampton SO17 1BJ, UK*

Received 12 May 2010; revised 26 May 2010; accepted 29 May 2010
Available online 4 June 2010

A systematic study of hydrogenated amorphous silicon nitride films deposited by varying gas flow rate ratio ($R = SiH_4/NH_3$) using Photo-Chemical Vapour Deposition reveal that as R is increased, dominant phase changes from silicon oxynitride to silicon nitride with embedded silicon nanoclusters. The change in photoluminescence spectral features in these films is attributed to quantum confinement effect. The results suggest that hydrogen plays a crucial role in overall phase evolution and in-situ formation of Si nanoclusters embedded in silicon nitride matrix.

Keywords: Silicon nitride; Phase stabilization; Silicon nanocrystals; Photoluminescence

Amorphous and crystalline silicon nanoclusters are of great interest in silicon photonics due to their efficient light emission as compared to bulk silicon [1]. Post-deposition thermal treatment of silicon-rich silicon dioxide (SiO_2) or Si_3N_4 films, which are mostly deposited using the CMOS-compatible plasma-enhanced chemical vapour deposition (PECVD) technique [2–5], is traditionally used to grow silicon nanostructures.

Although the SiO_2 matrix has been used as a typical matrix for silicon nanocrystals (Si-NC), Si_3N_4 has recently been the object of attention as an attractive alternative, especially for optoelectronic applications [6–8]. a-SiN_x:H generally exhibits strong room-temperature photoluminescence (PL) and electroluminescence, both in the visible as well as in the ultraviolet spectral regions [9–12]. Although the origin of PL is still not unambiguously understood, many reports separately attributed observation of violet to red PL to either a quantum confinement related effect of Si-NC or to radiative recombination between localized band-tail states caused by defects [13–16].

However, complete control over PL, to establish a Si-based full-color emitter, is far from being established due to the lack of information available to correlate PL to influential factors such as the presence of different phases (SiO_xN_y, SiO_2, SiN_x and Si) and the inadvertent presence of hydrogen (H) especially in a-SiN_x:H films. In addition, recent studies have attributed growth of Si-NC in silicon nitride matrix to H incorporation due to using ammonia instead of nitrogen [8,17]. The interactions between H atoms originating during the deposition process and various phases in a-SiN_x:H matrix can control the microstructure of the film structure and critically influence optical properties. Therefore in the present work the relevance of H concentration to evolution of various phases and the in-situ growth of Si-NC in as-deposited a-SiN_x:H thin films, deposited by the Hg-sensitized photo-CVD technique for different gas flow rate ratios, i.e. ($R = SiH_4/NH_3$), is presented.

The a-SiN_x:H films were deposited on n-type (1 0 0) crystalline Si substrates at 200 °C by photo-CVD (SAMCO UVD-10, Japan). In this set-up mercury vapour was introduced into the reaction chamber by passing the reactant gases through a mercury reservoir located out-

* Corresponding author. Tel.: +91 11 2659 1326; fax: +91 11 2658 1114; e-mail: prakash@physics.iitd.ac.in
[1] Currently at: Valencia Nanophotonics Technology Center, Universidad Politécnica de Valencia, 46022 Valencia, Spain.

1359-6462/$ - see front matter © 2010 Acta Materialia Inc. Published by Elsevier Ltd. All rights reserved.
doi:10.1016/j.scriptamat.2010.05.049

side the chamber with provision for heating up to 200 °C. The UV radiation at 254 nm emitted from a low-pressure mercury lamp is resonantly absorbed by mercury vapour and hence transfers energy to the reactant gases [18]. Argon-diluted SiH_4 (4%) and NH_3 were used as the precursor, and the gas flow rate ratio, $R = (SiH_4/NH_3)$, was varied from 0.04 to 0.57. Spectroscopic ellipsometry was carried out at an incidence angle of 75° in the range 400–900 nm and the corresponding ellipsometric angles; psi (Ψ) and delta (Δ) were fitted using a spline model to obtain optical constants, i.e. refractive index (n) and extinction coefficient (k). X-ray photoelectron spectroscopy (XPS) measurements were carried out to evaluate surface composition, using a SPECS system, equipped with a Mg K_α (1253.6 eV) source. Binding energy corrections were done using the carbon peak (284.6 eV) as a reference. All spectra were recorded after sputtering the samples for 3 min with 5 keV Ar ions. Elastic recoil detection analysis (ERDA) technique was used to determine the hydrogen concentration (C_H) in the as-deposited a-SiN_x:H samples using Ag^{7+} (100 MeV) ions from a 15 MV Pelletron accelerator. PL measurements at room temperature were carried on these films with 405 nm (CW) diode laser with a power density of ~1 W cm^{-2} as an excitation source. High-resolution transmission electron microscopy (HRTEM) was used to confirm the formation and determine the of Si-NC.

Figure 1a and b shows typical ellipsometric data and corresponding optical constants, i.e. refractive index (n) and extinction coefficient (k), as a function of wavelength. The inset of Figure 1b shows a monotonic increase in the refractive index with an increase in R-value, suggesting formation of non-stoichiometric a-SiN_x:H films. An increase in the value of refractive index of a-SiN_x:H films is due to an increase in the chemical bonds in the order Si–Si > Si–H > Si–N > N–H [19]. However, reported n-values may be slightly different from actual ones due to process-induced H incorporation [20]. Furthermore, the non-zero k-values (0.02–0.034) are a consequence of strongly absorbing weak Si–Si bond formation as revealed by an increase in the value of the refractive index [21].

To demonstrate the change in surface composition, Figure 2a and b show XPS data for the films of two extreme R-values: 0.04 and 0.50. Figure 2a shows Si 2p

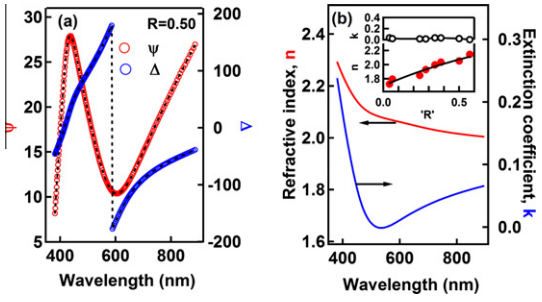

Figure 1. (a) Ellipsometer parameters Ψ and Δ experimental and fitted values using a spline model for the film $R = 0.50$. (b) Optical constants: refractive index (n) and extinction coefficients (k) vs. wavelength plot obtained from ellipsometric analysis. Inset shows n and k (at 633 nm) values plotted as a function of R.

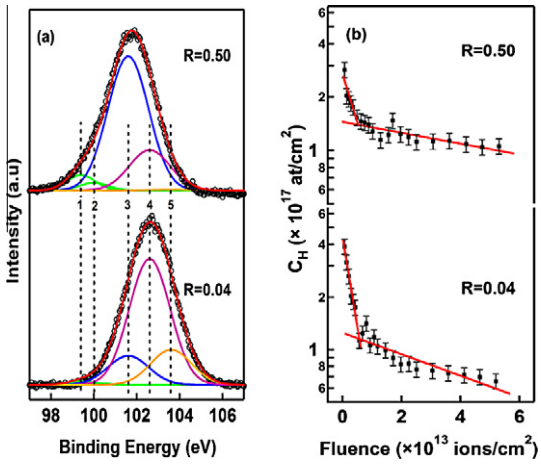

Figure 2. Representative XPS spectra for the as-deposited films corresponding to $R = 0.04$ and 0.50. (a) Deconvoluted Si 2p XPS spectra: peaks 1 and 2 correspond to elemental Si, whereas peaks 3, 4 and 5 represent Si in Si_3N_4, SiO_xN_y and SiO_2 networks, respectively. (b) Variation of hydrogen concentration (C_H) with fluence: solid lines (red) are linear fits.

core level spectra, which spans from 98 to 105 eV. It is an indication for the coexistence of varying ionic states of Si atoms, thus fitting was done as adopted by Kärcher et al. [22]. As seen from Figure. 2a, the binding energy spectra are typically composed of various Si phases, i.e. unreacted Si, Si_3N_4, SiO_xN_y and SiO_2.

For the lower R-value, the surface composition is typically dominated by SiO_xN_y and SiO_2 phases, and as R increases, the Si_3N_4 phase becomes stabilized. In addition, the peak around 99.5 ± 0.1 eV, which is a fingerprint of elemental Si, is clearly observed for the film corresponding to the higher R-value. This result unambiguously suggests that phase separation is already under way, with nearly stoichiometric Si_3N_4 as the dominant phase. One can also observe that the peaks of intermediate energies that correspond to sub-nitride species are progressively disappearing as R increases. Therefore, XPS results clearly demonstrate that c-Si/a-Si and phases approximating Si_3N_4 are dominant in films with higher R-values, which is in accordance with the ellipsometry measurements. In addition to this, the O 1s XPS spectrum (not shown here) clearly reveals O- and H-deficient structure in $R = 0.50$ as compared to $R = 0.04$ films.

In our previous study it was speculated that that a mere increase in R would not result in Si-rich a-SiN_x:H films, but that the H content during deposition plays a vital role in the overall phase evolution of the host matrix. It was proposed that less incorporation of H in as-deposited films with moderate Si content helps in the stabilization of silicon nitride (Si_3N_4) phase and may also enable unreacted Si atoms to cluster [20]. Since it not possible to quantify H concentration using O 1s XPS spectra, ERDA measurements were used to estimate H concentration (C_H), adopting the method discussed in our earlier work [20]. Figure 2b shows the variation in C_H for $R = 0.04$ and 0.50 films as a function of fluence. The estimated H concentration (C_H divided by film thickness) for $R = 0.04$ and 0.50 films are 3.58 and 2.40 ($\times 10^{22}$ atoms cm^{-3}), respectively. By compar-

ing XPS and ERDA measurements, one may conclude that lower H content favors phase stabilization and Si nanocluster formation, which corroborates our earlier and present experimental findings [20].

We have performed HRTEM analysis for as-deposited a-SiN_x:H films to validate our results. Figure 3a is the typical HRTEM image along with the selected-area electron diffraction (SAED) pattern, suggesting the formation of silicon clusters. Although Si-NC were not uniform in shape/size, the typical size of Si-NC was found to be ~5 nm. The enlarged view of the HRTEM image, notably the fringe contrast from (111) lattice planes (with $d_{(111)} = 0.23$ nm of Si) further confirms the Si crystalline phase formation. The PL spectra of all as-deposited films are displayed in Figure 3b. While the PL peak shows a marked red shift as R-value increases, films of $R = 0.04$ and 0.06 do not exhibit any PL within the detectable (500–1100 nm) range. Figure 3c shows that PL peak energies (solid circles) correspond to the Si-NC obtained from HRTEM analysis; a plot of the quantum confinement empirical model given in Ref. [17] is also used for comparison (dashed line). Assuming the above empirical model is completely applicable, correlation between PL peak energy and Si-NC size are in turn used to evaluate the Si-NC sizes (ranging between 3 and 5 nm) and the same are plotted as open circles.

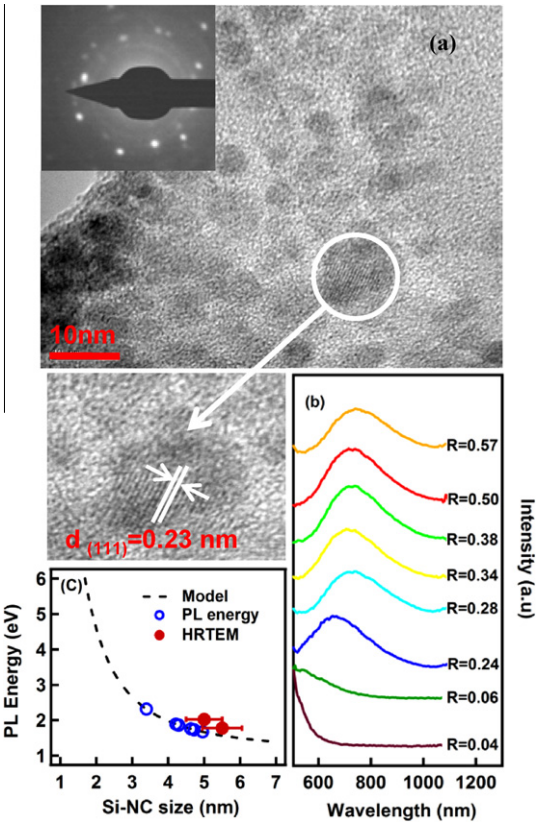

Figure 3. (a) HRTEM image along with SAED pattern for $R = 0.50$ film. (b) Room-temperature PL spectra for different R-values. (c) A plot of PL energy vs. Si-NC size: open circles represent the estimated Si-NC size [17] from the experimentally observed PL peak energies and solid circles are PL energies corresponding Si-NC sizes, obtained from HRTEM data. Dotted line is model plot [17] as a guide to eye.

To understand more about the PL data for $R = 0.04$ and 0.06 films, where the PL is at the blue side, let us revisit the phase evolution of as-deposited a-SiN_x:H. According to XPS data (Fig. 2a) for lower R-value, the films are predominantly SiO_xN_y with nominal phases of Si_3N_4, and SiO_2 and no signature of elemental Si, suggesting incorporation of oxygen into the films. Some oxygen incorporation is process induced as films are not deposited at very low pressures, however, such a large amount of oxygen incorporation could be due to presence of voids in these nitrogen-rich films. On further increasing the R-value, the probability of Si_3N_4 phase formation increases in accordance with secondary reactions of the photo-CVD. As the ammonia flow rate is decreased (in the ratio $R = SiH_4/NH_3$), the nitrogen is dispersed within the amorphous matrix, forming a more homogeneous silicon nitride phase, while the excess Si is clearly phase-segregated. Moreover, at higher R-values, the formation of SiO_2 phase (Fig. 2a) is minimal because of the strong diffusion barrier created by the more dominating Si–N bonding, which in turn prevents further oxidation [23]. Therefore, one may propose that appearance of unreacted Si in higher R-value films is a result of gradual evolution and modification of individual phases, i.e. Si_3N_4 and SiO_xN_y. One can further suggest that as R increases, the film becomes Si-rich because the formation of more stabilized silicon nitride phase creates more disorder since the nitrogen takes 3-fold coordination with silicon [24]. In addition to this, under thermodynamic equilibrium, the formation of Si–NH–Si bonds instead of N–Si_3 bonds by active H leads to stress relaxation in a-SiN_x:H films [25]. Several model mechanisms, including the partial equilibrium model, the surface diffusion model, the selective etching model and the chemical annealing model, have been proposed to discuss the role of H in chemically induced disorder-to-order structural transformations and crystallization in a-Si:H films at temperatures much lower than those required for thermal annealing [26,27]. The aforementioned experimental observations indicate that the strain produced by the formation of silicon nitride phase and excess silicon undergoes disorder-to-order structural relaxation via the insertion of H into the matrix. Subsequently, during the deposition process as H moves away, the bonds are broken, leading to rearrangements in the network resulting in equilibrium bond lengths and bond angles close to those of c-Si [28]. Therefore in-situ formation of the Si-NC can be understood as a result of a combination of the release of disorder-induced stress and the phase transition from amorphous Si to Si-NC induced by active H under suitable conditions.

Finally, let us discuss the origin of PL from the phase evolution point of view. Kato et al. have reported that a-SiO_xN_y:H and a-SiN_x:H films exhibit a similar broad PL with a peak energy around 2.2–2.9 eV due to radiative recombination between localized band-tail states associated with Si–N bonds [23]. According to theoretical calculation, the PL peak at 2.3 eV originates from $\equiv Si^0 \rightarrow = N^-$ transitions, and it has also been reported to exist at 2.4 eV due to oxygen defects [29,30]. A peak at 1.75 eV has been reported due to the luminescence from Si-NC, and band-tail-related PL generally occurs between 2.6 and 2.9 eV [31,32]. Furthermore, Wang et

al. empirically proposed that the PL observed using a 325 nm excitation would be preferentially due to N- and Si-related defects [33]. In addition, it is well known from the theoretical model that PL position of the defects is almost fixed and cannot be controlled [34]. Therefore, considering all aforementioned possibilities, the PL variation for the films above $R = 0.24$, where the peak is systematically red-shifting from 1.67 to 2.30 eV, could be attributed to quantum confinement-related effects [17]. Moreover the observed PL at room temperature without annealing the as-deposited a-SiN_x:H films is due to the formation of Si-NC in silicon nitride matrix and thereafter passivation of dangling bonds by H as revealed by the presence of H in the as-deposited a-SiN_x:H films by ERDA. However, further studies are needed to rule out completely the presence of non-radiative defect centres.

In summary, we have demonstrated in-situ growth of Si-NC in a-SiN_x:H film deposited by photo-CVD. The tunability of emission observed in as-deposited a-SiN_x:H film strongly indicates that the origin of light emission is determined by size-dependent quantum confinement effects as well as by the phases present. The ammonia flow rate served to modulate the structural evolution of the silicon nitride film containing Si-NC and eventually its size. The present experimental findings suggest that for phase separation to occur, the amount of incorporated H should be least in the as-deposited a-SiN_x:H film. The formation of in-situ Si nanoclusters embedded in as-deposited a-SiN_x:H films and the amorphous-to-nanocrystalline transformation is driven by a combination of chemical annealing and disorder-to-order structural relaxation through active hydrogen.

We acknowledge help from the personnel at the XPS, HRTEM and ERDA facilities of IIT Delhi and IUAC, New Delhi. This work is partially supported by the UK–India Education and Research Initiative (UKIERI) project.

[1] L. Pavesi, L. Dal Negro, M. Cazzanelli, G. Pucker, Z. Gaburro, G.V. Prakash, G. Franzò, F. Priolo, SPIE proceedings (Photonic West) 4293 (2001) 162.
[2] G. Vijaya Prakash, N. Daldosso, E. Degoli, F. Iacona, M. Cazzanelli, F. Rocca, Z. Gaburro, P. Dalba, C.E. Moreira, D. Pacifici, G. Franzò, F. Priolo, C. Arcangeli, A.B. Filonov, S. Ossicini, L. Pavesi, J Nanosci. Nanotech. 1 (2001) 159.
[3] L. Khriachtchev, T. Nikitin, C.J. Oton, R. Velagapudi, J. Sainio, J. Lahtinen, S. Novikov, J. Appl. Phys. 104 (2008) 104316.
[4] R.T. Neal, M.D.C. Charlton, G.J. Parker, C.E. Finlayson, M.C. Netti, J.J. Baumberg, Appl. Phys. Lett. 83 (2003) 4598.
[5] R.T. Neal, M.E. Zoorob, M.D. Charlton, G.J. Parker, C.E. Finlayson, J.J. Baumberg, Appl. Phys. Lett. 84 (2004) 2415.
[6] P. Bettoti, M. Cazzanelli, L. Dal Negro, B. Danesi, Z. Gaburro, C.J. Otón, G. Vijaya Prakash, L. Pavesi, J. Phys: condens. Matt. 14 (2002) 8253.
[7] Y.Q. Wang, Y.G. Wang, L. Cao, Z.X. Cao, Appl. Phys. Lett. 83 (2003) 3474.
[8] T.Y. Kim, N.M. Park, K.H. Kim, G.Y. Sung, Y.W. Ok, T.Y. Seong, C.J. Choi, Appl. Phys. Lett. 85 (2004) 5355.
[9] R. Carius, K. Jahn, W. Siebert, W. Fuhs, J. Lumin. 31 (1984) 354.
[10] W.A. Jackson, T.M. Searle, I.G. Austin, J. Non-Cryst. Sol. 77 (1985) 909.
[11] R.C. Fang, Y.Z. Song, M. Yang, W.D. Jiang, J. Non-Cryst. Sol. 77 (1985) 913.
[12] V.A. Gritsenko, K.S. Zhuravlev, A.D. Milov, H. Wong, R.W.M. Kwok, J.B. Xu, Thin Solid Films 353 (1999) 20.
[13] H.L. Hao, L.K. Wu, W.Z. Shen, Appl. Phys. Lett. 92 (2008) 121922.
[14] N.M. Park, C.J. Choi, T.Y. Seong, S.J. Park, Phys. Rev. Lett. 86 (2001) 1355.
[15] S.V. Deshpande, E. Gulari, S.W. Brown, S.C. Rand, J. Appl. Phys. 77 (1995) 6534.
[16] K. Yamaguchi, K. Mizushima, K. Sassa, Appl. Phys. Lett. 77 (2000) 3773.
[17] T.W. Kim, C.H. Cho, B.H. Kim, S.J. Park, Appl. Phys. Lett. 88 (2006) 123102.
[18] V.K. Rathi, M. Gupta, R. Thangaraj, K.S. Chari, O.P. Agnihotri, Thin Solid Films 266 (1995) 219.
[19] J.W. Lee, R. Ryoo, M.S. Jhon, K.I. Cho, J. Phys. Chem. Solids. 56 (1995) 293.
[20] S.P. Singh, P. Srivastava, S. Ghosh, S. Khan, G. Vijaya Prakash, J. Phys.: Condens. Matter. 21 (2009) 095010.
[21] S. Kohli, J.A. Theil, P.R. McCurdy, P.C. Dippo, R.K. Ahrenkiel, C.D. Rithner, P.K. Dorhout, Thin Solid Films 516 (2008) 4342.
[22] R. Kärcher, L. Ley, R.L. Johnson, Phys. Rev. B. 30 (1984) 1896.
[23] S. Wolf and R. N. Tauber, Silicon Processing for the VLSI Era, Lattice, Sunset Beach, CA, 1, 1986, pp. 210.
[24] H. Kato, N. Kashio, Y. Ohki, K.S. Seol, T. Noma, J. Appl. Phys. 93 (2003) 239.
[25] S. Hasegawa, Y. Amano, V. Inokuma, Y. Kurata, J. Appl. Phys. 75 (1994) 1493.
[26] R.C. Mani, I. Pavel, E.S. Aydil, J. Appl Phys. 102 (2007) 043305.
[27] I. Kaiser, N.H. Nickel, W. Fuhs, W. Pilz, Phys. Rev. B. 58 (1998) R1718.
[28] V. Sriraman, S. Agarwal, E.S. Aydil, D. Maroudas, Nature 418 (2002) 62.
[29] J. Robertson, M.J. Powell, Appl. Phys. Lett. 44 (1984) 415.
[30] T. Kanashima, M. Okuyama, Y. Hamakawa, Jpn. J. Appl. Phys. 35 (1996) 1445.
[31] S. Kohli, J.A. Theil, P.C. Dippo, K.M. Jones, M.M. Al-Jassim, R.K. Ahrenkiel, C.D. Rithner, P.K. Dorhout, Nanotechnology 15 (2004) 1831.
[32] T. Noma, K.S. Seol, H. Kato, M. Fujimaki, Y. Ohki, Appl. Phys. Lett. 79 (2001) 1995.
[33] M. Wang, D. Li, Z. Yuan, D. Yang, V. Que, Appl. Phys. Lett. 90 (2007) 131903.
[34] B.H. Kim, C.H. Cho, T.W. Kim, N.M. Park, G.Y. Sung, S.J. Park, Appl. Phys. Lett. 86 (2005) 091908.